

Production and measurements of individual single-wall nanotubes and small ropes of carbon

Sivaram Arepalli,^{a)} Pavel Nikolaev, and William Holmes
*G. B. Technologies, Incorporated/Lockheed Martin, P. O. Box 58561, Mail Stop C61,
 Houston, Texas 77258*

Bradley S. Files
National Aeronautics Space Administration, Johnson Space Center, Houston, Texas 77058

(Received 7 November 2000; accepted for publication 6 January 2001)

This work focuses on the size and spatial dependence of single-wall carbon nanotubes produced by the pulsed-laser vaporization technique. The study indicates that very long (tens of microns) individual nanotubes form in the vicinity of the target, and subsequently coalesce into bundles. The role of the inner flow tube is confirmed to restrict plume expansion and improve interactions between carbon atoms resulting in nanotube and rope formation. The effect of the flowing buffer gas seems to influence the dispersion of particulate contaminant material in the nanotube product. More particulate matter is produced at lower oven temperatures. © 2001 American Institute of Physics. [DOI: 10.1063/1.1352659]

Recently, there has been much active interest in the production, processing, manipulation, and incorporation of carbon nanotubes to improve properties of materials.^{1–6} Carbon nanotubes are normally found as ropes/bundles of single-wall or multiwall tubes. Most of the current work is on single-wall nanotubes (SWNTs) because of their superior thermal, mechanical, and electrical properties compared to multiwall nanotubes, resulting in many possible applications.^{4–6} Lack of reliable sources of pure SWNTs prompted several researchers to modify existing production processes to improve quantity as well as quality of SWNTs. Also, emphasis is being put on developing methods to improve the purity⁷ of the SWNT samples, which seem to be critical for most applications. It is also realized that understanding growth mechanisms may help produce SWNTs of higher purity and known properties.^{8–10} Specific applications may call for SWNTs of certain length, diameter, or chirality.^{1,11} Determining these fundamental properties may require advanced instrumentation [atomic force microscopy (AFM), scanning electron microscopy (SEM), transmission electron microscopy (TEM), scanning tunneling microscopy, Raman, etc.] and include electron diffraction methods.¹² Measurement of the lengths of the tubes is more important in the design of nanotube composite materials. For these materials to be reinforced mechanically by the tubes, issues of critical length and aspect ratio are critical. Opinions in the research community on the length of nanotubes vary. One school of thought is that the nanotubes are intrinsically short (<500 nm) and agglomerate into longer tubes and bundles during production as well as dispersion in solvents. Seemingly infinite bundle length is irrelevant to the lengths of nanotubes comprising it. It is impossible to follow and measure individual nanotubes in a bundle, which can be built of rather short tubes. Bundles have to be separated in order to observe and measure individual tubes. Some researchers

have tried to infer the length of nanotubes by chromatographic methods,¹³ AFM and from scattering methods.¹⁴ These results show tubes that may be too short after processing to be useful in composites.

The goal of this work is to measure the lengths of nanotubes as formed, without further processing. AFM is a convenient way to measure lengths and diameters of tubes and bundles,¹⁵ but specimen preparation has always involved SWNT dispersion in solvents and subsequent deposition on suitable substrates,^{13,14} which may very well affect SWNT bundling. In order to be able to look at pristine SWNTs, “witness plates” (optical quality quartz flats and microscope slides) were placed at different locations in the laser oven. The laser shutters were then opened for a very short time, producing sparse nanotubes scattered on the substrates. It appears that the roughness of such substrates is worse than normally used mica or silicon, but still completely adequate, and nanotubes bind well enough to allow AFM imaging. This provided an opportunity to make AFM measurements of the nanotubes without further processing. Finding the right exposure times was important, since too many nano-

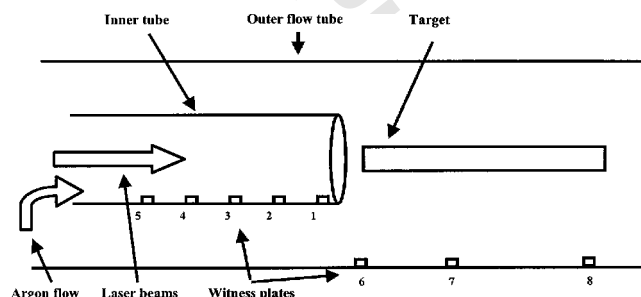


FIG. 1. Witness plates located inside the flow tube of the laser oven set up. Positions 1–5 collect the nanotubes formed upstream of the target which is 6 mm away from the edge of the inner tube. Argon gas flow and laser beams are directed near the center of the flow tube. In the case of “no inner tube”, the witness plates are placed at the bottom of the outer flow tube at the same axial-distances from the target.

^{a)} Author to whom correspondence should be addressed;
 electronic mail: sivaram.arepalli1@jsc.nasa.gov

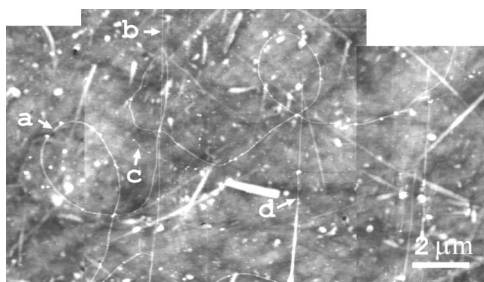


FIG. 2. AFM image of plate No. 3 exposed for 0.5 s, without inner tube and argon flowing at 100 sccm. (a) Individual tube, 1.25 nm diameter and $>22 \mu\text{m}$ long. (b) Individual tube, 0.86 nm diameter, $>18.01 \mu\text{m}$ long. (c) Short tube, 0.8 nm diameter, $0.38 \mu\text{m}$ long. (d) Tapered bundle.

tubes on the substrate form a spongy mat-like coating unsuitable for AFM. Conversely, if there are not enough tubes, they are difficult to find.

Our pulsed-laser vaporization setup, which is described in an earlier communication,⁹ now utilizes two 60 Hz lasers with a green pulse followed by IR within 50 ns. Argon flow of 100 sccm at 500 Torr is directed through the 25 mm inner tube located inside a 55 mm flow tube placed in a tubular oven. Five witness plates were placed 1.8 cm apart inside the inner tube starting 1.2 cm from the target. Three more witness plates were placed at the bottom of the outer flow tube, one right underneath the target and the others 6 and 17 cm down stream from the target (Fig. 1). Once the laser furnace was running, the laser beam shutters were opened briefly to deposit nanotubes onto the plates. Three sets of plates were collected at room temperature, and exposed for 0.5, 5, and 35 s, respectively. A fourth set was collected at a furnace temperature of 773 K for 0.5 s. Sets five through seven were collected at 1473 K with a 0.5 s exposure under standard run conditions, and under run conditions with the gas flow stopped and without the inner tube.

The witness plates were removed and imaged using AFM. A Digital Instruments Nanoscope IIIa at Rice University was operated in the tapping mode using $125 \mu\text{m}$ long TESP tips. Typically sixteen $5 \mu\text{m} \times 5 \mu\text{m}$ scans forming an overlapping 4×4 frame mosaic were made on each witness plate, and images of larger areas were recorded to follow longer nanotubes. The height resolution is about 0.1 nm, and

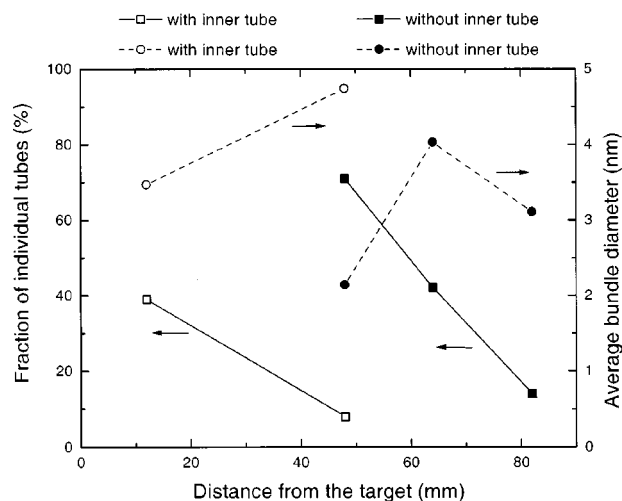


FIG. 4. Fraction of the individual nanotubes and average bundle thickness dependence on the distance from the target for runs with and without inner tube at 1473 K.

the substrate smoothness was satisfactory to allow easy imaging of individual nanotubes and bundles.

Runs at 1473 K have produced some nanotubes close to the target (plate Nos. 1, 2, and 3 with the inner tube and plate Nos. 3, 4, and 5 without the inner tube) and almost nothing on the rest of the witness plates (Fig. 2). Statistics on lengths and diameters obtained from AFM measurements are presented in Fig. 3. Most nanotubes and bundles are so long that it is impossible to follow them all the way to their ends. Other nanotube ends are often buried in piles of nanoparticles.¹⁶ Thus, it is important to emphasize that most length measurements are lower estimates, and nanotubes are definitely longer, possibly much longer.

Far from the target we see almost exclusively bundles, while close to the target we see a significant fraction of individual tubes, and the bundles are generally much thinner (Fig. 4). This shows that tubes form within the ablation plume and propagate away from the target as it expands. As they fly away, they collide with each other and form bundles; hence more bundles and thicker bundles are found farther away from the target. Relative numbers of individual nanotubes versus bundles deposited on the plates is always higher

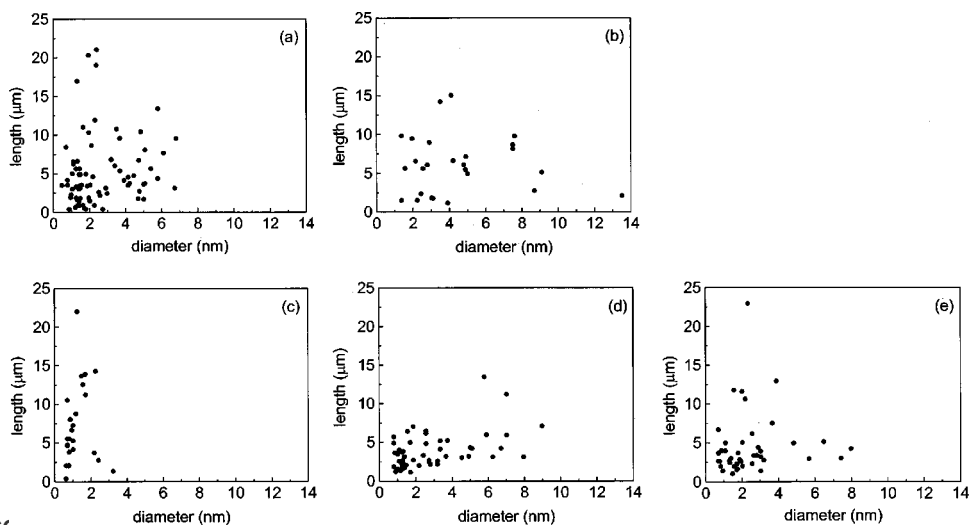


FIG. 3. Diameters and lengths of nanotubes in 1473 K runs: (a) and (b): with inner tube, plate Nos. 1 and 3. (c), (d), and (e): without inner tube, plate Nos. 3, 4, and 5.

in experiments without the inner tube. In the presence of the inner tube, the volume into which the plume expands is smaller. Therefore, the number density of nanotubes is higher, increasing the likelihood of tubes colliding with each other and forming bundles. Thus, more and thicker bundles are produced with the inner tube. Another difference is that with the inner tube nanotubes deposit on plate Nos. 1, 2, and 3 and without it on plate Nos. 3, 4, and 5. This happens because in the absence of the inner tube the expanding plume carrying nanotubes comes in contact with substrates farther upstream from the target.

An important observation is that individual nanotubes as long as $20\ \mu\text{m}$ deposit as close as 12 mm from the target. Since the plume expands with about 100 m/s velocity,⁹ we can estimate the nanotube growth rate to be at least ~ 0.15 m/s, assuming that they grow uniformly as they travel straight ahead towards the first plate.

Several researchers^{13,14} observe much shorter nanotubes after some form of chemical and/or ultrasonic processing and/or purification. We have to conclude that such processing significantly shortens nanotubes.

Observed diameters and lengths will probably differ in the case of a 5–6 h production run. Indeed, argon flow in the inner tube moves only about 8 mm in 0.5 s, meaning that nanotube number density does not reach the equilibrium that would be attained in a production run. Therefore, long production runs must produce almost exclusively bundles of nanotubes, which indeed is normally observed.

Running at 1473 K with stopped flow produced too many particles¹⁶ on substrates to allow AFM imaging; nevertheless, nanotubes and bundles were seen in about the same abundance as in experiments with flow. The reason for seeing more particles on substrates with no argon flow is unclear. It is very unlikely that relative amounts of produced nanotubes and particles have changed. Relatively slow (~ 1.5 cm/s) argon flow is not likely to affect the nanotube production in the laser plume expanding at ~ 100 m/s. However, the absence of argon flow may influence the spatial distribution of “heavy” particles and “light” nanotubes as they deposit on the substrates.

As the oven temperature is decreased to 773 and 293 K, we see a huge increase in the amount of particulate matter mixed with nanotubes. Nanotubes are still there, as evident from the SEM images of the substrate No. 6 exposed for 35 s at room temperature (Fig. 5). But it is virtually impossible to see them in AFM, since particles obscure nanotubes and make imaging impossible. It is well established that nanotube yield decreases with furnace temperature, and our observations confirm this trend. Unfortunately, this has precluded us from obtaining any data on the nanotube length versus temperature.

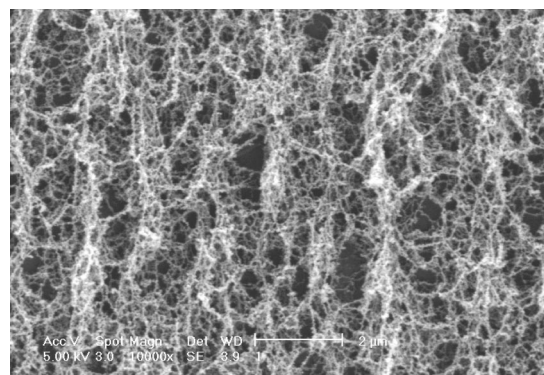


FIG. 5. SEM image of plate No. 6 exposed for 35 s at room temperature.

In conclusion, the current measurements indicate the formation of long individual nanotubes and their coalescence into ropes. The role of the inner tube is confirmed to control the expansion of the ablated plume and help their coalescence into bundles.

The authors wish to acknowledge helpful support and encouragement from B. Hauge and R. Smalley. Access to equipment at the Center for Nanoscale Science and Technology (CNST), Rice University is appreciated.

¹ B. I. Yakobson and R. E. Smalley, *Am. Sci.* **85**, 324 (1997).

² C. Dekker, *Phys. Today* **52**, 22 (1999).

³ R. Andrews, D. Jacques, A. M. Rao, T. Rantell, F. Derbyshire, Y. Chen, and R. C. Haddon, *Appl. Phys. Lett.* **75**, 1329 (1999).

⁴ B. S. Files and B. M. Mayeaux, *Adv. Mater. Processes* **156**, 47 (1999).

⁵ R. Saito, G. Dresselhaus, and M. S. Dresselhaus, *Physical Properties of Carbon Nanotubes* (Imperial College Press, London, 1998).

⁶ M. S. Dresselhaus, G. Dresselhaus, and P. C. Eklund, *Science of Fullerenes and Carbon Nanotubes* (Academic, San Diego, CA, 1996).

⁷ K. D. Ausman, R. Piner, O. Lourie, and R. S. Ruoff, *J. Phys. Chem. B* **104**, 8911 (2000).

⁸ A. C. Dillon, P. A. Parilla, J. I. Alleman, J. D. Perkins, and M. J. Heben, *Chem. Phys. Lett.* **316**, 13 (2000).

⁹ S. Arepalli, P. Nikolaev, W. Holmes, and C. D. Scott, *Appl. Phys. A: Mater. Sci. Process.* **70**, 125 (2000).

¹⁰ M. Yudasaka, R. Yamada, N. Sensui, T. Wilkins, T. Ichihashi, and S. Iijima, *J. Phys. Chem. B* **103**, 6224 (1999).

¹¹ A. C. Dillon, K. M. Jones, T. A. Bekkedahl, C. H. Kiang, D. S. Bethune, and M. J. Heben, *Nature (London)* **386**, 377 (1997).

¹² L. Henrard, A. Loiseau, C. Journet, and P. Bernier, *Eur. Phys. J. B* **13**, 661 (2000).

¹³ R. S. Duesberg, J. Muster, V. Krastic, M. Burghard, and S. Roth, *Appl. Phys. A: Mater. Sci. Process.* **67**, 117 (1998).

¹⁴ J. Liu, A. G. Rinzler, H. Dai, J. H. Hafner, R. K. Bradley, P. J. Boul, A. Lu, T. Iverson, K. Shelomov, C. B. Huffman, F. Rodriguez-Macias, Y.-S. Shon, T. R. Lee, D. L. Colbert, and R. E. Smalley, *Science* **280**, 1253 (1998).

¹⁵ C. Lieber, *Solid State Commun.* **107**, 607 (1998).

¹⁶ Observed nanoparticles range 5–50 nm in size, and are either graphite or graphitized catalyst particles (from TEM observations).